



# *Evaluation of Microfluidic Biosensor Development Using Microscopic Analysis of Molecular Beacon Hybridization Kinetics*

Chuanwu Xi,<sup>1</sup> Lutgarde Raskin,<sup>1</sup>  
and Stephen A. Bopp<sup>2,\*</sup>

<sup>1</sup>Department of Civil and Environmental Engineering,

<sup>2</sup>Department of Electrical and Computer Engineering,

Department of Bioengineering, University of Illinois at Urbana-Champaign, Beckman Institute for Advanced Science and Technology, Urbana, IL 61801, USA

E-mail: bopp@uiuc.edu

**Abstract.** Molecular beacons, oligonucleotide probes that fluoresce upon hybridization to a target nucleic acid, can be used in microfluidic devices to detect and quantify nucleic acids in solution as well as inside bacterial cells. Three essential steps towards the development of such devices as integrated microfluidic biosensors using molecular beacons were investigated in the present study. First, experiments using real-time confocal microscopy indicated that diffusion of DNA molecular beacons across a 100- $\mu\text{m}$  diameter microfluidic channel took less than one minute after the flow of reagents was stopped. Second, experiments to evaluate hybridization kinetics of DNA molecular beacons with target nucleic acids in solution showed that DNA molecular beacons can be used to characterize hybridization kinetics in real time in microfluidic channels and that hybridization signals approached their maximum in approximately three minutes. Finally, it was demonstrated that peptide nucleic acid molecular beacons can be used to detect bacterial cells in microfluidic devices. These results suggest that the use of microfluidic devices to detect nucleic acids in solution and in bacterial cells is promising and that further development of an integrated microfluidic biosensor for bacterial detection based on this concept is warranted.

**Key Words.** molecular beacon, peptide nucleic acid, hybridization kinetics, microfluidic biosensor

## **1. Introduction**

Microfluidic devices have attracted a great deal of attention during the past several years because of their wide application in biology and biotechnology (Figeys and Pinto 2000; Harrison et al., 1993; Mitchell 2001). Although the fabrication and use of microfluidic devices has been highly successful, the understanding of flow phenomena and biochemical reaction kinetics in these systems is still limited because of the lack of appropriate analysis tools. In the past, several methods have been used to characterize flow phenomena in microfluidic devices including light microscopy (Therriault et al., 2003), confocal microscopy (Liu et al., 2000; Stroock et al., 2002), laser particle velocimetry (Grant, 1997; Meinhart et al., 1999), fluorescence correlation spectroscopy (Brinkmeier et al., 1999; Dittrich and Schwille, 2002) and optical coherence

tomography (Schaefer et al., 2004; Xi et al., 2004). However, few studies have investigated real-time biochemical reaction kinetics in microfluidic devices (Kamholz et al., 1999; Liu et al., 2000).

A molecular beacon (MB) is a single-stranded oligonucleotide that only fluoresces upon hybridization to its target nucleic acid (Tyagi et al., 1998; Tyagi and Kramer 1996). A DNA MB consists of a probe sequence flanked by two complementary sequences (Figure 1A), which allows formation of a stem-loop structure when the MB is free in solution. A reporter fluorophore is attached to one end and a quencher to the other end, which results in quenching of fluorescence when both ends are in close proximity (in the absence of target nucleic acids). The fluorophore provides a signal when the MB opens its stem to hybridize to a target sequence. Therefore, MBs can be used to detect specific DNA or RNA sequences in an aqueous solution without the prerequisite of immobilizing either the target nucleic acid or the probe as in traditional hybridization assays or in DNA microarrays. In addition, the wash steps that typically are needed post-hybridization to remove unbound probes can be eliminated. These properties should make MBs ideal for studying flow phenomena and biochemical kinetics in real time in microfluidic channels.

Peptide nucleic acid (PNA) is a DNA analogue with a polyamide backbone instead of a sugar phosphate backbone (Egholm et al., 1993). Recently, we used DNA and PNA MBs to detect and quantify rRNA in solution and in whole cells. We found that PNA MBs are ideal tools for bacterial whole cell detection in solution and in real time (Xi et al., 2003). In the present study, we used real-time confocal microscopy to detect the fluorescence emitted from DNA and PNA MBs in microfluidic systems. Real-time confocal microscopy detection of DNA and PNA MBs was used to evaluate mixing and diffusion, to

\*Corresponding author.

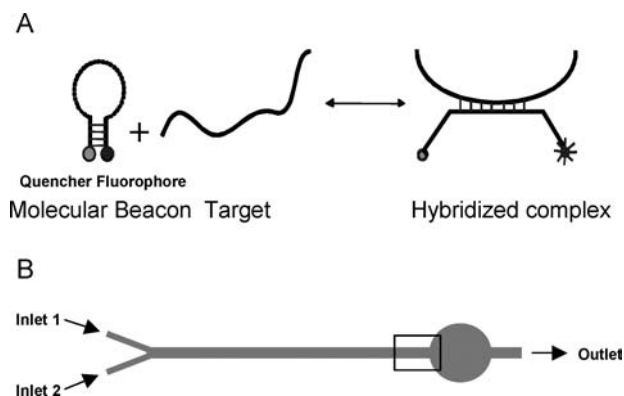


**Fig. 1.** (A) Schematic of MB hybridization. A DNA MB consists of a probe sequence flanked by two complementary sequences, which allow formation of a stem-loop structure when the MB is free in solution. A reporter fluorophore is attached to one end and a quencher attached to the other end quenches the fluorescence when both ends are in close proximity, in the absence of target nucleic acids. The fluorophore provides a signal when the MB hybridizes to a target sequence and opens its stem. (B) Diagram of the microfluidic device (mixer) used in this study. The box indicates the position at which fluorescence signal was collected.

characterize hybridization kinetics, to detect and quantify ribosomal RNA (rRNA), and to detect bacterial cells in a representative microfluidic device.

## 2. Materials and Methods

### 2.1. Molecular beacons and biological materials

DNA MB Bact0338 (Fluorescein-5'-CATCCGCTGCCTCCCGTAGGAGTG-3'-DABCYL) and PNA MB Bact0338 (Fluorescein-E-GCTGCCTCCCGTAGGA-K-K-DABCYL) were synthesized by Megabases Inc. (Evanston, IL) and Applied Biosystems (Mountain View, CA), respectively. The probe sequences (indicated in bold) are complementary to a conserved region in the 16S rRNA of most *Bacteria* (positions 338-355 and 338-353 *Escherichia coli* numbering for DNA MB Bact0338 and PNA MB Bact0338, respectively). Details on the design and fabrication of these DNA and PNA MBs were described previously (Xi et al., 2003).

A DNA oligonucleotide complementary to the probe region of DNA MB Bact338 (5'-ACTCCTACGGGAGGCAGC-3') and a DNA oligonucleotide with one mismatch (5'-ACTCCTACGCGAGGCAGC-3', mismatch indicated in bold) were synthesized by Megabases, Inc. (Evanston, IL) and were used to evaluate hybridization kinetics. Total RNA, containing the target 16S rRNA, was extracted from a pure culture of *E. coli* strain Dh5 $\alpha$  harvested during the mid-log growth phase. For whole cell hybridization, pure cultures of *E. coli* harvested during stationary phase were fixed with 4% paraformaldehyde

for 2 hours as described previously (Raskin et al., 1994).

### 2.2. Microfabrication and use of microfluidic devices

The microfluidic devices were fabricated using polydimethyl siloxane (PDMS) as previously described (Balberg et al., 2000; Jo et al., 2000). The layout of the Y-shaped microfluidic device is shown in Figure 1B. The main channel is 100  $\mu\text{m}$  in width and 1 cm in length. The two input channels are 50  $\mu\text{m}$  in width. All channels are 100  $\mu\text{m}$  deep. Oxygen plasma was applied to the channel surfaces by placing the PDMS microfluidic device in a reactive-ion-etching (RIE) plasma chamber. A flow of pure oxygen and an RF field of 70 W were applied for 20 seconds (Jo et al., 2000). MBs and target nucleic acids were injected into the input channels of the microfluidic device using syringe pumps (WPI 200i, WPI, Aston, UK).

### 2.3. Hybridization and fluorescence measurement

Hybridizations of DNA MBs with DNA oligonucleotides were performed in a hybridization buffer consisting of a 10-mM phosphate buffer (pH 7.8), 900 mM NaCl, 1.3% polyethylene glycol (PEG), and 30% formamide (referred to as NaCl/PEG hybridization buffer) (Hristova et al., 2000). A hybridization buffer containing 25 mM Tris-HCl and 100 mM NaCl amended with 40% formamide was used for experiments with PNA MBs (referred to as Tris-HCl/NaCl hybridization buffer) (Xi et al., 2003). All hybridization experiments were performed at room temperature. Fluorescence emissions were acquired and imaging was performed using a confocal laser scanning microscope (Leica, TCS SP2, Wetzlar, Germany). The excitation was performed at a wavelength of 488 nm and emission was detected using a filter set for fluorescein at a wavelength of 515 nm. Images were assembled, displayed, and analyzed using commercial software (Leica Confocal Software).

## 3. Results

### 3.1. Visualization of DNA MB diffusion across a microfluidic channel in real time

To investigate mixing efficiency inside the microfluidic channel, 500  $\mu\text{l}$  each of 250 nM of DNA MBs and 250 nM of DNA oligonucleotides were mixed in a microcentrifuge tube for 2 hours at room temperature to form DNA hybrids. The DNA hybrid was injected into one input channel and the NaCl/PEG hybridization buffer into the second inlet. Figure 2 shows diffusion of the DNA hybrid in the final section of the main channel (indicated by the box in Figure 1B) from 0 to 60 seconds after the flow of 30  $\mu\text{l}/\text{min}$  had been stopped. These results indicate that complete

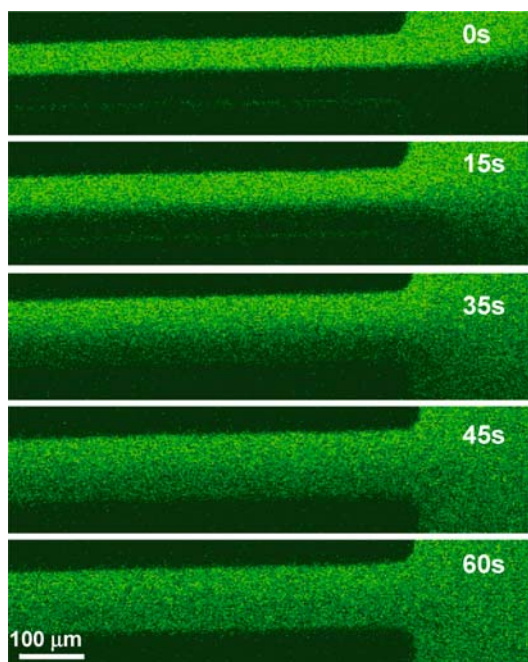


**Fig. 2.** Diffusion of hybridized MBs. Confocal microscopy images of the end of the main channel (box in Figure 1B) at different time points after the flow had been stopped, show mixing by diffusion.

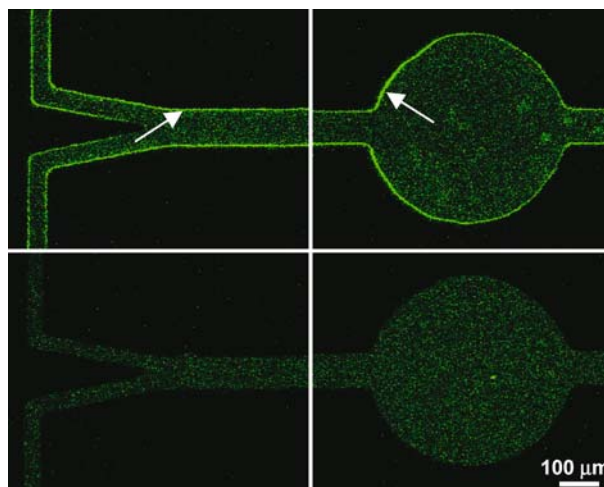
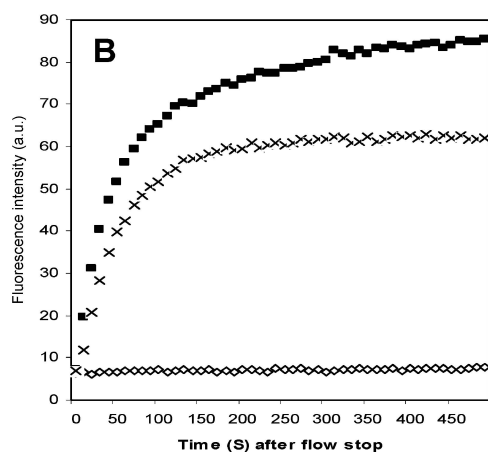
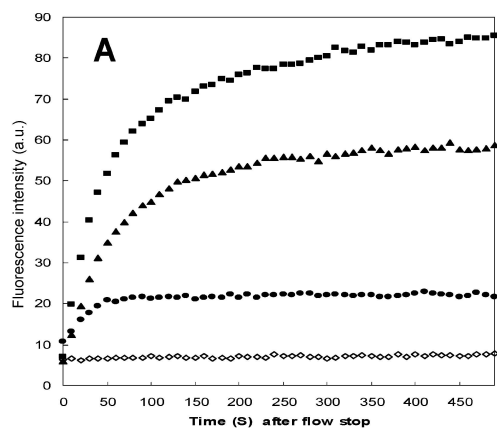


**Fig. 4.** Confocal microscopy images of two locations in the PDMS microfluidic channel injected with solutions of PNA MB Bact0338. Images are from a microfluidic device without (top) and with (bottom) oxygen plasma treatment. The devices without oxygen plasma treatment show absorption of PNA MBs on the PDMS surfaces (arrows).

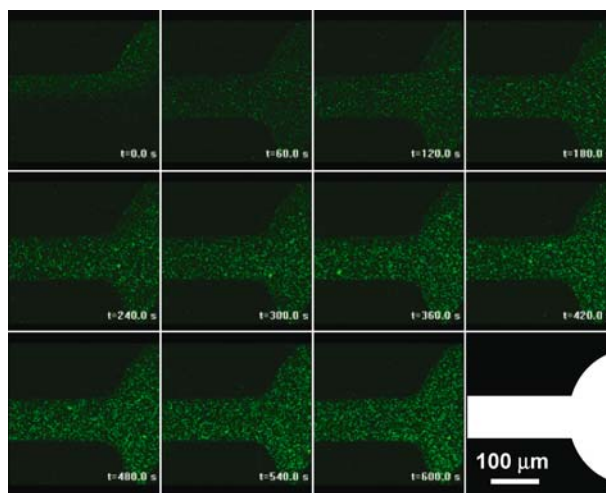


**Fig. 5.** PNA MB hybridization to *E. coli* cells. Series of confocal microscopy images of the end of the microfluidic channel at different time points after the flow had been stopped. A schematic of the microfluidic channel is included in the lower right corner of the image.

**Fig. 3.** DNA MB hybridization kinetics. Fluorescence intensity variation over time in the channel after flow had been stopped. (A) Hybridization of DNA MB Bact0338 (125 nM) with its target oligonucleotide at different concentrations (Filled square, 125 nM; Filled triangle, 80 nM; Filled diamond, 12.5 nM; Open diamond, no target). (B) Hybridization of DNA MB Bact0338 (125 nM) with its target oligonucleotide (Filled square, 125 nM), with an oligonucleotide with one mismatch (Cross, 125 nM), and control (Open diamond, no target).

mixing was achieved in less than one minute after the flow had been stopped (for a flow rate of 30  $\mu\text{l}/\text{min}$ ).

### 3.2. Hybridization kinetics of DNA MB with DNA oligonucleotides

To study the hybridization kinetics of MBs in microfluidic channels, solutions of DNA MB Bact0338 (250 nM) and different concentrations of DNA oligonucleotide target (250 nM, 160 nM, and 25 nM) or a DNA oligonucleotide with one mismatch (250 nM) were injected into the channel through the two inlets at flow rates of 5  $\mu\text{l}/\text{min}$ . The end of the channel was scanned every 10 seconds after the flow had been stopped. Imaging continued for 500 seconds. As a control, a 250-nM solution of MBs and the NaCl/PEG hybridization buffer solution were injected into the channel as described above and the end of the channel was scanned at the same rate. The fluorescence intensity at one point inside the channel was quantified and plotted versus time, as shown in Figure 3.

The results show that the fluorescence signal reached a plateau at approximately 200 seconds, indicating that the hybridization reaction was very fast in the channel. The fluorescence signal increased faster when the target concentration was higher (Figure 3A), indicating that the rate was target concentration dependent, as anticipated. Also, the maximum fluorescence intensity collected after 500 seconds increased in a linear fashion with the oligonucleotide target concentration (data not shown).

For the oligonucleotide with one mismatch, the fluorescence signal increased less during the first 75 seconds and the final fluorescence intensity was about 30% less compared to that of the perfect match target (Figure 3B). This result was expected since hybrids between DNA MBs and oligonucleotides with one mismatch are less stable than those formed between DNA MBs and target oligonucleotides.

### 3.3. Detection of *E. coli* cells in a microfluidic channel using PNA MBs

We showed in a previous study that PNA MBs performed better than DNA MBs to detect bacterial cells using whole cell hybridization (Xi et al., 2003), which prompted us to explore the use of PNA MBs for whole cell detection in microfluidic devices. When a solution of PNA MB Bact0338 was injected into a microfluidic channel, a fluorescent layer was observed on the surfaces of PDMS channels, which was brighter than the fluorescence of the solution in the channels (Figure 4). The accumulation of PNA MBs on the PDMS surface was likely due to the hydrophobic characteristics of PNA MBs and PDMS. To demonstrate this, solutions of PNA MBs and DNA MBs were injected into PDMS microfluidic channels that were either untreated or were treated with oxygen plasma prior

to addition of the MBs. Oxygen plasma treatment of the PDMS channel has been shown to increase its surface hydrophilicity (Duffy et al., 1998; McDonald et al., 2000). PNA MBs readily accumulated on the surfaces of untreated PDMS channels (Figure 4, top), showing a bright fluorescent layer. We did not observe this phenomenon when a solution of PNA MBs was injected into the PDMS channel treated with oxygen plasma (Figure 4, bottom). Similarly, the bright fluorescent layer was not seen when a solution of DNA MBs was injected into a PDMS channel, whether it was treated with oxygen plasma or not (data not shown). Since the absorption of PNA MBs to the PDMS surfaces is likely to affect hybridization kinetics by decreasing the concentration of PNA MBs in solution inside the channel, the PDMS channels used with PNA MBs were treated with oxygen plasma.

In order to evaluate the potential to detect bacterial cells in real time in a microfluidic channel, solutions of PNA MBs Bact0338 (250 nM) in Tris-HCl/NaCl buffer and fixed *E. coli* cells ( $10^9$  cells/ml) were injected into the microfluidic device through the two inlets at flow rates of 5  $\mu\text{l}/\text{min}$ . The end of the mixing channel was scanned once a minute after the flow had been stopped for a total of 60 minutes. As a control, a solution of PNA MBs (250 nM) and a buffer solution were injected into the microfluidic channel as described above and the end of the channel was scanned at the same rate. Approximately one minute after the flow had been stopped, the PNA MBs had diffused across the channel (i.e., from the upper part of the channel to the lower part of the channel) as shown by the appearance of background fluorescence due to the presence of the PNA MB (Figure 5,  $t = 60.0$  s). This rate of diffusion is similar to that for DNA MBs (Figure 2). After one minute, a few strong green fluorescent spots appeared in the center of the channel, indicating *E. coli* cells in this region started to fluoresce due to hybridization of their 16S rRNA with PNA MBs (Figure 5,  $t = 60.0$  s). The strong green fluorescent spots appeared in regions closer and closer to the upper edge of the channel from one minute to nine minutes after the flow had been stopped (Figure 5,  $t = 60.0$  s to  $t = 540.0$  s), indicating *E. coli* cells had diffused from the lower part to the upper part of the channel and PNA MBs hybridized to the 16S rRNA targets in these cells. Approximately ten minutes after the flow had been stopped, PNA MB-labeled *E. coli* cells also began to appear along the edges of the channel (Figure 5,  $t = 600.0$  s), indicating *E. coli* cells required approximately ten minutes to diffuse across the whole channel.

The hybridization signal, measured as average fluorescence intensity for the complete channel, increased relatively rapidly after the flow had been stopped and reached a maximum after approximately 40 minutes (Figure 6), indicating that the hybridization of PNA MB with 16S rRNA in whole bacterial cells was relatively fast. The

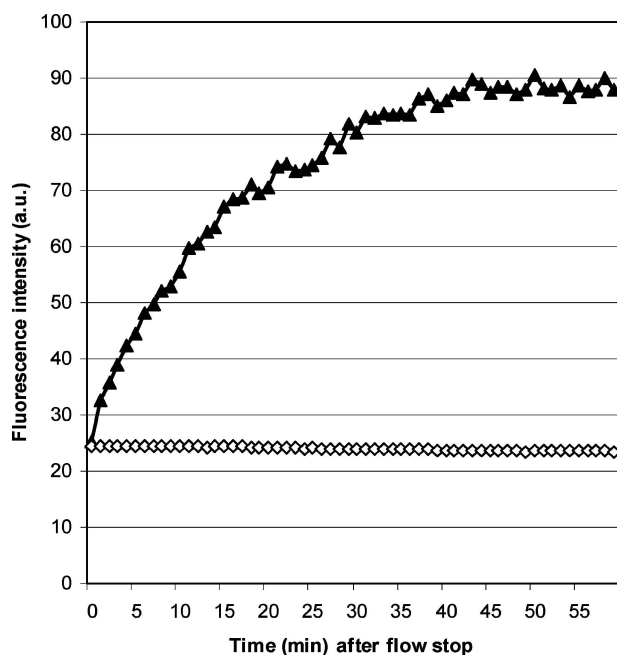


**Fig. 6.** PNA MB whole cell hybridization kinetics. Fluorescence intensity variation over time in the channel after the flow had been stopped. Hybridization of PNA MB Bact0338 (250 nM) with *E. coli* cells ( $10^9$  cells/ml, filled triangle). Open diamond, control without *E. coli* cells.

hybridization rate observed in this study was higher than the rate determined for a hybridization in a larger volume (microcentrifuge tube of 200  $\mu$ l) (Xi et al., 2003), for which the fluorescence intensity reached a maximum in about 60 minutes.

#### 4. Discussion and Concluding Remarks

In this study, real-time confocal microscopy and MBs were used to characterize diffusion and reaction kinetics in a microfluidic channel. Efficient mixing is a prerequisite for most biochemical reactions. Therefore, it is important to characterize and, if necessary, to improve the mixing efficiency in microfluidic channels. This study showed that mixing through diffusion is efficient for stop-flow reactions in microfluidic devices. In a related study, we characterized mixing patterns in more complex microfluidic devices designed for enhancing mixing under continuous flow conditions (Xi et al., 2004).

Taking advantage of the optical and biochemical properties of MBs, it was possible to monitor hybridization kinetics in microfluidic devices in real time. Previous studies have shown it is possible to model diffusion and reaction kinetics in microfluidic channels (Hatch et al., 2001; Schilling et al., 2002). Although beyond the scope of the current study, the development of a model that incorpo-

rates diffusion and MB hybridization kinetics for the microfluidic devices presented in this study would make it possible to quantify target molecules using MB hybridization by using a few data points collected at the beginning of a hybridization experiment, rather than waiting until the hybridization reaction would have reached completion. This approach would save a great deal of time when multiple hybridizations need to be performed in sequence and suggests that further development of a real-time, integrated biosensor based on the concepts developed in this study is warranted.

The use of PNA MBs versus DNA MBs allows the detection of targets with a high level of secondary and higher order structure, such as rRNA (Xi et al., 2003). We demonstrated that this approach can be used for the rapid detection of bacterial cells (through targeting their 16S rRNA) in real-time in microfluidic devices. Confocal microscopy of PNA MB hybridization in PDMS-based microfluidic devices revealed unwanted absorption of PNA MBs on PDMS surfaces, which was corrected by reactive ion-etching of the devices in an oxygen environment.

This research characterized diffusion efficiency, hybridization kinetics, and whole cell detection in microfluidic channels, which are essential steps when developing microfluidic biosensors for the detection of pathogenic and other bacteria. The methods developed in this study allow the omission of steps commonly needed in other biosensors, such as isolation of target DNA or RNA and target amplification with the polymerase chain reaction (PCR). The integration of nucleic acid isolation and PCR steps in microfluidic devices often leads to systems and approaches that are complex, difficult to control, and time consuming. In conclusion, this research provides a strong basis for the further development of a simple microfluidic biosensor for the rapid and specific detection of bacterial cells. Additional research on sample collection and preparation and system integration is needed.

#### Acknowledgments

The authors thank Michal Balberg for contributions during the early stages of this project. This work was supported by the U.S. National Science Foundation (BES-0086696, S. A. B.; CHE 01-03447, S. A. B.). Additional information can be found at <http://nb.beckman.uiuc.edu/biophotonics> and <http://cee.uiuc.edu/research/raskin/>.

#### References

- M. Balberg, K. Hristova, D.J. Brady, D.J. Beebe, and L. Raskin, Proceedings of 1st Annual International IEEE-EMBS, Special Topic Conference on Microtechnologies in Medicine and Biology (Lyon, France, 2000).

- M. Brinkmeier, K. Dorre, J. Stephan, and M. Eigen, *Anal. Chem.* **71**, 609–616 (1999).
- P.S. Dittrich and P. Schuille, *Anal. Chem.* **74**, 4472 (2002).
- D.C. Duffy, J.C. McDonald, O.J.A. Schueller, and G.M. Whitesides, *Analytical Chemistry* **70**, 4974 (1998).
- M. Egholm, O. Buchardt, L. Christensen, C. Behrens, S.M. Freier, D.A. Driver, R.H. Berg, S.K. Kim, B. Norden, and P.E. Nielsen, *Nature* **365**, 566 (1993).
- D. Figeys and D. Pinto, *Anal. Chem.* **72**, 330A (2000).
- I. Grant, *Proceedings of the Institution of Mechanical Engineers Part C—Journal of Mechanical Engineering Science* **211**, 55 (1997).
- D.J. Harrison, K. Fluri, K. Seiler, Z.H. Fan, C.S. Effenhauser, and A. Manz, *Science* **261**, 895 (1993).
- A. Hatch, A.E. Kamholz, K.R. Hawkins, M.S. Munson, E.A. Schilling, B.H. Weigl, and P. Yager, *Nat. Biotechnol.* **19**, 461 (2001).
- K. Hristova, M. Balberg, D. Frigon, M. Mau, D.J. Brady, D.J. Beebe, and L. Raskin, *Abstract Book of 100th General Meeting of American Society for Microbiology* (Los-Angeles, CA, 2000).
- B.H. Jo, L.M. Van Lerberghe, K.M. Motsegood, and D.J. Beebe, *Journal of Microelectromechanical Systems* **9**, 76 (2000).
- A.E. Kamholz, B.H. Weigl, B.A. Finlayson, and P. Yager, *Anal. Chem.* **71**, 5340 (1999).
- R.H. Liu, M.A. Stremler, K.V. Sharp, M.G. Olsen, J.G. Santiago, R.J. Adrian, H. Aref, and D.J. Beebe, *Journal of Microelectromechanical Systems* **9**, 190 (2000).
- J.C. McDonald, D.C. Duffy, J.R. Anderson, D.T. Chiu, H. Wu, O.J. Schueller, and G.M. Whitesides, *Electrophoresis* **21**, 27 (2000).
- C.D. Meinhart, S.T. Wereley, and J.G. Santiago, *Experiments in Fluids* **27**, 414 (1999).
- P. Mitchell, *Nat. Biotechnol.* **19**, 717 (2001).
- L. Raskin, L.K. Poulsen, D.R. Noguera, B.E. Rittmann, and D.A. Stahl, *Appl. Environ. Microbiol.* **60**, 1241 (1994).
- A.W. Schaefer, J.J. Reynolds, D.L. Marks, and S.A. Boppart, *IEEE Trans Biomedical Engr* **51**, 186 (2004).
- E.A. Schilling, A.E. Kamholz, and P. Yager, *Anal. Chem.* **74**, 1798 (2002).
- A.D. Stroock, S.K.W. Dertinger, A. Ajdari, I. Mezic, H.A. Stone, and G.M. Whitesides, *Science* **295**, 647 (2002).
- D. Therriault, S.R. White, and J.A. Lewis, *Nat. Materials* **2**, 265 (2003).
- S. Tyagi, D.P. Bratu, and F.R. Kramer, *Nat. Biotechnol.* **16**, 49 (1998).
- S. Tyagi and F.R. Kramer, *Nat. Biotechnol.* **14**, 303 (1996).
- C. Xi, M. Balberg, S.A. Boppart, and L. Raskin, *Appl. Environ. Microbiol.* **69**, 5673 (2003).
- C. Xi, D.L. Marks, D.S. Parikh, L. Raskin, and S.A. Boppart, *Proc. Natl. Acad. Sci. USA* **101**, 7516 (2004).